Hydrobiologia (2023) 850:4515–4530
https://doi.org/10.1007/s10750-022-05006-4

EFFECTS OF CHANGES IN SALINITY

# Photobiological and biochemical responses of mangrove-associated red macroalgae *Bostrychia calliptera* and *Bostrychia montagnei* to short-term salinity stress related to climate change

**Henrique D. S. Borburema · Angelika Graiff · Ulf Karsten · Eliane Marinho-Soriano**

Received: 31 May 2022 / Revised: 14 August 2022 / Accepted: 23 August 2022 / Published online: 13 September 2022


**Abstract** Salinization in tropical estuarine environments is expected as a result of climate change. The physiological performance of mangrove-associated key macroalgae can negatively be affected by increased salinity in such habitats. Thus, we analyzed photobiological and biochemical responses of the closely related red algae *Bostrychia calliptera* and *Bostrychia montagnei* incubated under a range of salinities (5, 11, 18, 37, 47, and 57 $S_A$). Effective and maximum quantum yield, relative electron transport rate vs. photon fluence rate curves, photosynthetic parameters, and complementary energy dissipation pathways indicated that both species had lower photosynthetic performance under increased salinity, which was more strongly pronounced in *B. calliptera*. Both species increased their organic osmolyte contents with rising salinity stress. Dulcitol was the main organic osmolyte synthesized by *B. calliptera*, whereas *B. montagnei* synthesized dulcitol and sorbitol. Our results demonstrate that increased salinity in estuaries due to climate change will be detrimental to photosynthesis of both macroalgae, with *B. calliptera* more affected than *B. montagnei*. As *B. montagnei* synthesizes both dulcitol and sorbitol, it is more tolerant to salinity stress compared to *B. calliptera*. Our data document for the first time a new organic osmolyte distribution pattern in *Bostrychia* species, namely the occurrence of dulcitol only.

**Keywords** Dulcitol · Estuarine salinization · Global change · Osmolytes · Photosynthetic performance · Salinity tolerance · Sorbitol

Guest editors: Erik Jeppesen, Miguel Cañedo-Argüelles, Sally Entrekin, Judit Padisák & S.S.S. Sarma / Effects of induced changes in salinity on inland and coastal water ecosystems

**Supplementary Information** The online version contains supplementary material available at https://doi.org/10.1007/s10750-022-05006-4.

H. D. S. Borburema (✉) · E. Marinho-Soriano
Department of Oceanography and Limnology, Federal University of Rio Grande do Norte, Via Costeira, Mãe Luiza, Natal, RN 59014-002, Brazil
e-mail: henrique.borburema@ufrn.edu.br; henrique.tpb@gmail.com

A. Graiff · U. Karsten
Institute of Biological Sciences, Applied Ecology and Phycology, University of Rostock, Albert-Einstein-Strasse 3, 18059 Rostock, Germany

## Introduction

Increased greenhouse gas concentrations in the Earth's atmosphere due to the anthropogenic activities have resulted in climate change worldwide (IPCC, 2019). The Intergovernmental Panel on Climate Change (IPCC) projects for tropical zones of the Atlantic and of Northeastern South America a decrease in precipitation for 2081–2100 relative to 1986–2005 (IPCC, 2014). Semi-arid and arid climate

regions in tropics and subtropics will experience much less precipitation and runoff due to the longer dry periods (Collins et al., 2013). Such changes will result in reduced freshwater input into coastal aquatic ecosystems, such as estuaries, which will lead to less salt dilution in estuarine waters (Rybczyk et al., 2012). Climate change has also already resulted in sea level rise in tropical Atlantic (IPCC, 2019) due to thermal expansion of seawater and the melting of glaciers and ice caps in high latitudes (Collins et al., 2013). Sea level rise will lead to the expansion of coastal flooding areas, resulting in increased saltwater intrusion into estuaries (Rybczyk et al., 2012). Moreover, it will push estuarine zones upslope making them narrower (or wider) depending on topography, rainfall, and freshwater inflows. Human water removal in the watershed, especially during major droughts in semi-arid regions, is also a serious problem to drive estuarine salinization. In addition, higher evaporation rates are expected in estuaries of tropical zones due to further warming, resulting in increased salt conditions in these environments. Thus, salinization is expected in tropical estuarine environments influenced by semi-arid climate as a result of drought, sea level rise, and warming (Rybczyk et al., 2012; Bindoff et al., 2019).

In tropical and subtropical estuarine environments, mangrove forests represent the typical and most abundant vegetation type worldwide (Giri et al., 2011). In mangrove forests, red macroalgae of the genera *Caloglossa* (Harvey) G. Martens, *Catenella* Greville, and mainly *Bostrychia* Montagne form an intertidal association termed Bostrychietum (Post, 1936). These macroalgae grow as epiphytes on prop-roots, trunks, and pneumatophores of mangrove trees of the genera *Rhizophora* L., *Laguncularia* C. F. Gaertn, and *Avicennia* L. (West et al., 1992; Pedroche et al., 1995). Along with microalgae, these red algae represent a relevant source of primary productivity in mangrove ecosystems (Karsten et al., 1994a, 2000) and can contribute to $CO_2$ sequestration (Kieckbusch et al., 2004; Borburema et al., 2022a). The Bostrychietum is a relevant microhabitat for several invertebrates (García et al., 2016; Vieira et al., 2018; Borburema et al., 2021) and can be used as bioindicator of environmental quality (Melville & Pulkownik, 2006, 2007; Rios-Marin et al., 2021). In tropical and subtropical Brazilian mangroves, among the *Bostrychia* species, *Bostrychia calliptera* (Montagne) Montagne and *Bostrychia montagnei* Harvey occur with high predominance (Yokoya et al., 1999b; Cunha & Costa, 2002a; Fontes et al., 2007; Machado & Nassar, 2007; Mendonça & Lana, 2021).

By inhabiting estuarine ecosystems, where the salinity is a key environmental factor that varies temporally and spatially, *Bostrychia* species are tolerant to salinity variations (e.g., Karsten & Kirst, 1989a, b; Karsten et al., 1994a, b; Borburema et al., 2020; Sánchez de Pedro et al., 2022). As a physiological strategy to maintain the turgor pressure of the cells under osmotic stress due to increased salinity, *Bostrychia* species synthesize and accumulate the polyols dulcitol and sorbitol (low molecular weight carbohydrates) as organic osmolytes (e.g., Karsten & Kirst, 1989b; West et al., 1992; Karsten et al., 1994a, b, 1996a, b; Sánchez de Pedro et al., 2016; Gambichler et al., 2021a). The effects of salinity variation on *Bostrychia* species have been well investigated and documented in the scientific literature. However, Brazilian specimens have been poorly studied in terms of salinity tolerance (e.g., Cunha & Duarte, 2002b; Borburema et al., 2020, 2022b). Commonly, high salinities negatively affect nutrient uptake (e.g., Choi et al., 2010; Carneiro et al., 2020), growth (e.g., Karsten et al., 1993; Yokoya et al., 1999a; Pereira et al., 2017), and photosynthesis of macroalgae (e.g., Choi et al., 2010; Gambichler et al., 2021a). Furthermore, hypersaline conditions in the external medium affect macroalgae in two ways: first, the water potential is strongly reduced leading to dehydration of cells, and secondly, high concentrations of inorganic ions such as sodium and chloride exert toxic effects on cellular metabolism (Karsten, 2012). Physiological processes in the algal photosynthetic pathways are usually inhibited under high salinities (Kirst, 1990). For example, the photoactivation of electron flow at the reducing site of photosystem I, the electron flow at the water splitting site of photosystem II, and the transfer of light energy among pigment complexes (Kirst, 1990).

Currently, several studies have explored the effects of different environmental stressors on the algal photosynthesis using in vivo chlorophyll *a* fluorescence measurements as proxies for photosynthetic performance (e.g., Scherner et al., 2013, 2016; Celis-Plá et al., 2015; Figueroa et al., 2019; Graiff et al., 2021; Nauer et al., 2021, 2022). In this perspective, Sánchez de Pedro et al. (2022) and Borburema et al. (2022a)

investigated photosynthetic parameters of *Bostrychia* species under desiccation stress and ocean acidification, respectively. In those studies, *Bostrychia scorpioides* Hudson (Montagne) decreased its photosynthetic performance under increased desiccation stress (Sánchez de Pedro et al., 2022) and the photosynthetic performance of *B. calliptera* and *B. montagnei* in general was not affected by ocean acidification (Borburema et al., 2022a). For *Bostrychia* species subjected to salinity variation, in vivo chlorophyll *a* fluorescence measurements were only measured by Gambichler et al. (2021a) and Borburema et al. (2022b) to estimate the maximum and effective quantum yield in photosystem II, respectively.

In the present study, we analyzed photobiological responses and organic osmolyte contents (dulcitol and sorbitol) of the mangrove-associated key macroalgal species *B. calliptera* and *B. montagnei* from a tropical estuarine environment of Brazil influenced by semi-arid climate. These taxa were incubated under rising salinities to test the hypotheses: (i) increased salinity in estuaries due to climate change will be detrimental to macroalgal photosynthesis; (ii) both species will exhibit osmotic acclimation to compensate the increase in salinity by synthesizing and accumulating organic osmolytes, dulcitol and sorbitol; and (iii) based on a previous study (Borburema et al., 2022b), *B. calliptera* will show a lower physiological performance than *B. montagnei* under increased salinity.

## Materials and methods

### Collection site, algal collection, and unialgal cultures

Thalli of *Bostrychia calliptera* and *B. montagnei* were collected in the mangrove swamp of Mamanguape River Estuary Environmental Protection Area (6° 46′ 15.00″ S and 34° 56′ 15.00″ W), Paraíba state, Brazil, in September 2021. Based on Köppen Climate Classification System, the climate of the coast of Paraíba state is tropical humid and hot (Alvares et al., 2013). At the algal collection site only two seasons occur, a dry season from September to February (spring/summer), and a rainy season from March to August (autumn/winter) (Sassi et al., 1988). Moreover, the Paraíba state is located in Northeastern Brazil, a tropical semi-arid climate region where annual rainfall drops on average to less than 800 mm (Alvares et al., 2013). Thus, two-thirds of the Mamanguape river basin is influenced by the semi-arid climate, which causes an intermittent freshwater flow regime in most of the basin. The Northeastern part of Brazil suffered between 1990 and 2016 a sequence of drought years due to El Niño atypical events (Marengo et al., 2017). Surveys conducted in 2011 and 2014 already registered salinities in the Mamanguape river estuary higher than those documented by sampling carried out in 1997 and 2000 (Lima et al., 2020). Based on records made between 2007 and 2008 (Xavier et al., 2012), and between 2015 and 2016 (Lima et al., 2020), an increase in mean salinity of approximately five salinity units for the zone closest to the estuary mouth can be considered (during the dry season).

Both red algae were collected from prop-roots of *Rhizophora mangle* L. during low tide (0.1 m in height) in sites about 2 km from the estuarine mouth. In the Mamanguape river estuary, over a 24-h tidal cycle, low and high tides occur alternately every 6 h, and the amplitude of tidal movements ranges from 0.0 to 2.7 m. Tidal data were obtained from the nearest tide gauge (Cabedelo, 6° 58′ 0.2 S and 34° 50′ 0.4 W, https://www.marinha.mil.br/chm/tabuas-de-mare). As observed in field, over low tides, the Bostrychietum is fully emersed. Algal collection was authorized by ICMBio/Brazil (authorization nº 65168-1), since it was carried out within Brazilian conservation unit. During the field collection, most of the estuarine sediment was removed from the thalli with estuary water. The specimens were transported to the laboratory of marine macroalgae of Federal University of Rio Grande do Norte (Brazil) in thermally insulated boxes at a temperature of around 20°C and in darkness. In the laboratory, the remaining sediment adhered on the thalli was removed by several washing and spraying with UV-sterilized and filtered seawater. Thalli parts with filamentous macroalgae were removed by cutting with scalpels and macrofauna individuals were removed with tweezers, both under a stereomicroscope. Voucher specimens were deposited in the herbarium of the Environmental Research Institute, São Paulo, Brazil, with accession numbers SP 513836 and SP 513835 for *B. calliptera* and *B. montagnei*, respectively. After these procedures, the macroalgae were transported to the laboratory of Applied Ecology and Phycology of University of Rostock (Germany) in thermally insulated bags at a temperature of around 20°C and in darkness, for the establishment

of unialgal cultures and salinity experiment. Macroalgae were transported from Federal University of Rio Grande do Norte to University of Rostock among paper towels moistened with natural seawater (salinity of 32) during a journey of approximately 42 h.

The macroalgae (biomass around 5 g $l^{-1}$) were washed with deionized water, gently blotted dry with paper towels and maintained in continuous immersion in 1 l Erlenmeyer flasks containing 800 ml of culture medium. The culture medium consisted of natural seawater (adjusted absolute salinity of 30–32 $S_A$) sterilized by filtering and enriched with Provasoli's solution (PES/2) (Starr & Zeikus, 1993). The culture medium was bubbled continuously and replaced weekly for nutrient replenishment. Algae were maintained under a water temperature of 21–24°C (night/diurnal room temperature), a photon flux density of 160–190 µmol photons $m^{-2}$ $s^{-1}$ provided by cool-white fluorescent tubes (Osram L36W/840, Lumilux, Germany) and a light: dark cycle of 16: 8 h (Karsten et al., 1994a). Both algae remained in these conditions for a 7-week acclimation period, after which visibly healthy thalli were experimentally stressed under the different salinities. Photon flux density was measured with a quantum photometer (LI-250, LI-COR, USA) attached to an underwater LI-COR quantum sensor (US-SQS/L, Walz, Germany).

## Experiment with different salinities

Vegetative thalli of *B. calliptera* and *B. montagnei* were incubated for 72 h (Karsten et al., 1994a, b, 1996a) in a range of salinities: 5.1, 11.2, 18.4, 37.1, 47.1, and 57.3 $S_A$. Salinities from 5.1 to 37.1 were established according to salinities recorded in the Mamanguape river estuary (Lima et al., 2020). The hypersaline conditions of 47.1 and 57.3 $S_A$ were established according to salinities recorded in hypersaline estuaries of Northeastern Brazil fully influenced by semi-arid climate (Sales et al., 2018; Duarte et al., 2020; Gonçalves, 2020), where evaporation rates are higher than precipitation rates. For each salinity, incubations were made in six compartments of a 6-well culture plate (Costar®, Corning Incorporated, USA), and each compartment was filled with 10 ml of the respective culture medium. The culture medium was natural seawater sterilized by filtering and enriched with full strength of Provasoli's solution (PES). Treatments were established using twelve 6-well culture plates (six salinities × two species). Each replicate ($n = 6$) consisted of one branch (2–3 cm in primary axis length) with laterals of the macroalgae. The lowest experimental salinity was obtained by mixing sterilized natural seawater (11.2 $S_A$) with deionized water, and the increased salinities by adding a saline solution prepared with sterilized natural seawater and artificial sea-salt (hw-Marinemix® professional, Wiegandt, Germany). The saline solution was added through filtering (FP 30/0.2 CA-S filters—0.2 µm porosity, Whatman®, Germany) to sterilize it as well. Mixing natural seawater with deionized water to produce the lowest salinity did not affect the seawater pH, which varied from 8.47 to 8.50 among treatments. Seawater pH and salinity were measured using a pH electrode (SenTix 41, WTW, Germany) and a salinity probe (TetraCon® 325, WTW, Germany) connected to a universal meter (MultiLine P4, WTW, Germany). The water temperature, photon flux density, and photoperiod conditions during the experiment were the same as previously described for the unialgal cultures.

## Photosynthetic parameters

In vivo chlorophyll *a* fluorescence measurements were obtained from the different replicates ($n = 6$) using a Pulse Amplitude Modulated (PAM) fluorometer (PAM-2500, Walz, Germany) to calculate several photosynthetic parameters of the macroalgae. Before incubating the algae in different salinities, and every 24 h during the incubation, the effective quantum yield ($\Delta F/F_m'$) of photosystem II (PSII) was calculated. The formula $\Delta F/F_m' = (F_m' - F_t)/F_m'$ was used, where $F_t$ is the current steady-state fluorescence of light-adapted algae and $F_m'$ is the maximum fluorescence of the algae under actinic light during a saturating pulse (Schreiber et al., 1995). $F_t$ was measured under a very low photon fluence rate of red light (0.05 µmol photons $m^{-2}$ $s^{-1}$), and $F_m'$ . During the fluorescence measurements, the branches (2–3 cm in primary axis length) were placed in a glass Petri dish containing culture medium. The fluorescence measurements were always performed from the apical parts of the branches. Before incubating, they were performed with branches submersed in culture medium of the acclimation (described above), during and at the end of experiment they were performed

with branches submersed in their respective experimental culture media.

On the last experimental day, after measuring $F_t$ and $F_m'$ to calculate the effective quantum yield, the macroalgae were dark-acclimated for 15 min. Then, light pulses (2, 6, 64, 101, 141, 198, 271, 363, 474, 619, and 785 µmol photons $m^{-2}$ $s^{-1}$) were applied in 20 s intervals to construct relative electron transport rate (rETR) vs. photon fluence rate (PAR) curves. From the first light pulse the maximum quantum yield of PSII was calculated using the formula $F_v/F_m = (F_m - F_o)/F_m$, where $F_m$ is the maximum fluorescence during a saturating pulse on dark-acclimated algae, and $F_o$ is the basal fluorescence (Schreiber et al., 1995; Suggett et al., 2011). Relative electron transport rates were calculated by multiplying the quantum yield with the appropriate PAR values ($rETR = \Delta F/F_m' \times PAR$) (Schreiber et al., 1995; Suggett et al., 2011). Relative electron transport rate vs. photon fluence rate curves were fitted applying the mathematical model of Walsby (1997) ($R^2 = 0.99$), due to the presence of photoinhibition. From each curve, the maximum relative electron transport rate ($rETR_{max}$), the light utilization coefficient (α), the photoinhibition coefficient (β), and the initial saturation irradiance for photosynthesis ($I_k$) were calculated.

For each treatment, complementary energy dissipation pathways in PSII were investigated. The photochemical pathway was calculated as $Y(II) = (F_m' - F_t)/F_m'$, whereas the non-regulated non-photochemical quenching of light energy (Y[NO]) was determined using the formula $Y(NO) = F_t/F_m$, and the regulated non-photochemical quenching of light energy (Y[NPQ]) was calculated using the formula $Y(NPQ) = F_t/F_m' - Y(NO)$. The Y(NO) reflects the fraction of energy that is passively dissipated in form of heat and fluorescence, mainly due to closed PSII reaction centers, while Y(NPQ) corresponds to the fraction of energy dissipated in form of heat via the regulated photoprotective non-photochemical quenching mechanisms (Scherner et al., 2013). Overall, the total energy is conserved as $Y(II) + Y(NPQ) + Y(NO) = 1$.

## Dulcitol and sorbitol analyses by high-performance liquid chromatography

After incubating for 72 h, the macroalgae were washed with deionized water to remove the salt on the branches, gently blotted dry with paper towels, frozen in liquid nitrogen, and stored at − 20°C and in darkness for further dulcitol and sorbitol analyses by high-performance liquid chromatography (HPLC) (Karsten et al., 1991). Macroalgae were lyophilized in a freeze-drier (CDplus, Christ, Germany) and subsequently powdered using mortar and pestle. Dulcitol and sorbitol were extracted from the powdered algal samples (10 mg dry weight, $n = 6$) in 2 ml of aqueous 70% ethanol (v/v, HPLC grade) in a water bath (70°C) for 4 h. During the incubation time in the water bath, the samples were vortexed regularly (Vortex-Genie 2, Scientific Industries, USA) to optimize extraction. Afterward, samples were centrifuged at 13,000×*g* for 15 min (Biofuge pico, Heraeus, Germany) and the ethanolic supernatants transferred to new microtubes, followed by evaporation to dryness in a Speed Vacuum Concentrator (RVC 2–25, Christ, Germany). Subsequently, the dried pellets were re-dissolved in HPLC water (1.8 ml) in an ultrasonic bath (RK 510 H, Bandelin Sonorex, Germany) at 70°C for 30 min. Aqueous homogenates were vortexed for 30 s and then centrifuged at 13,000×*g* for 15 min. Finally, the aqueous supernatants were transferred to HPLC vials after passing through a 0.45 µm filter (Whatman™, Germany) prior injection onto the HPLC column.

Dulcitol and sorbitol in the samples were analyzed qualitatively and quantitatively using a 1260 Infinity HPLC system (Agilent Technologies, Germany) with a refractive index (RI) detector. A BIO-RAD Aminex Fast Carbohydrate Analysis Column HPAP (100 × 7.8 mm, 9 µm, BIO-RAD, USA) protected by a guard cartridge (Carbo-Pb 4 × 3 mm I.D., Phenomenex, Germany) was used to identify dulcitol and sorbitol. During measurements, the mobile phase (eluent) was pure HPLC water with a flow rate of 1 ml $min^{-1}$, 35 bar pressure, column temperature at 70°C, and 10 µl as the injection volume. The peaks in the chromatograms were identified by retention time and integrated manually. To quantify dulcitol and sorbitol in the samples, 10-point calibration curves were made based on standard solutions of both polyols with concentrations from 0.1 to 5 mM $l^{-1}$. Dulcitol and sorbitol concentrations were calculated using the integrated peak area and the slope of the calibration curves ($R^2 = 0.999947$ for dulcitol curve, and $R^2 = 0.999948$ for sorbitol curve). Osmolyte concentrations in the macroalgae were expressed as mmol per kg dry weight (mmol $kg^{-1}$ DW).

### Statistical analyses

The results are shown as the mean ± standard deviation (SD) based on six replicates per treatment. The physiological responses ($F_v/F_m$, α, β, $rETR_{max}$, $I_k$, Y[II], Y[NPQ], Y[NO], dulcitol, and sorbitol concentrations) measured at the end of the experiment were compared among treatments of salinity for each species by one-way analysis of variance (ANOVA) (Table S1). When significant differences were found ($P < 0.05$), Tukey's post hoc tests were applied. Non-parametric Kruskal–Wallis' tests followed by Dunn's post hoc tests were performed when the data did not show normality by the Shapiro–Wilk's test and homogeneity of variance by the Levene's test (Table S1). To compare the effective quantum yield ($\Delta F/F_m'$) among salinities over time (hours), two-way repeated-measures ANOVAs were performed for each species (Table S2). The comparisons between species were made applying Wilcoxon–Mann–Whitney's tests, except for $I_k$ and Y(NPQ). For these physiological responses, the student's *t* test was applied, since they showed normality and homogeneity of variance. All statistical analyses were performed using the R software (Version 4.0.3).

## Results

### Photobiological responses

*Bostrychia calliptera* exhibited a decreased $\Delta F/F_m'$ under salinities of 47.1 and 57.3 $S_A$ during the incubation time (Fig. 1A, Table S2). In addition, $\Delta F/F_m'$ also declined at 37.1 $S_A$ after 72 h of incubation (Fig. 1A). Under salinities of 5.1, 11.2, and 18.4 $S_A$, *B. calliptera* showed a similar $\Delta F/F_m'$ during the incubation time (Fig. 1A). *Bostrychia montagnei* also decreased its $\Delta F/F_m'$ under 47.1 and 57.3 $S_A$ during the whole incubation time (Fig. 1B, Table S2). Under salinities of 5.1, 11.2, 18.4, and 37.1 $S_A$, however, this species showed similar $\Delta F/F_m'$ values (Fig. 1B).

After 72 h of incubation under different salinities, both *B. calliptera* and *B. montagnei* exhibited a lower maximum quantum yield ($F_v/F_m$) under 47.1 and 57.3 $S_A$ (Tables 1, S1). *Bostrychia calliptera* also decreased its $F_v/F_m$ at 37.1 $S_A$ (Table 1). The $F_v/F_m$ did not differ significantly between species by the Wilcoxon–Mann–Whitney's test ($W = 638$, $P = 0.91$).

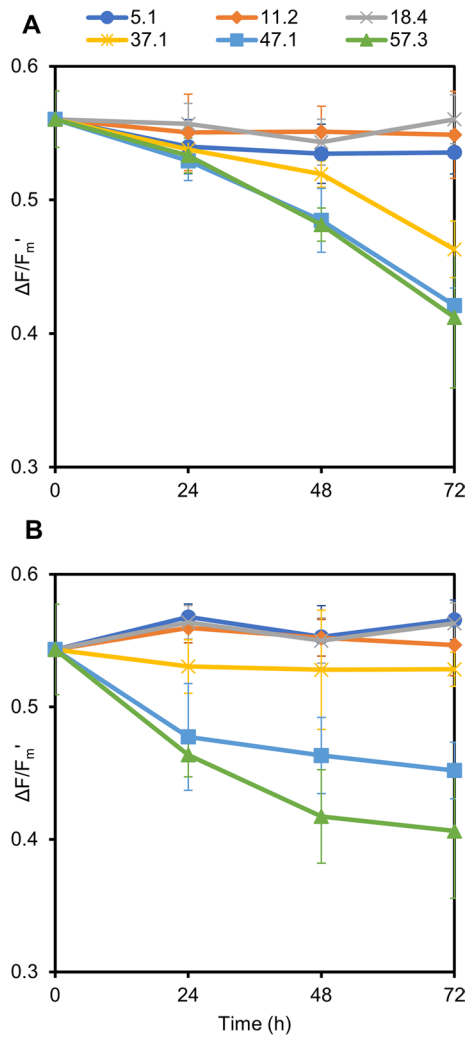


**Fig. 1** Effective quantum yield ($\Delta F/F_m'$) in photosystem II of *Bostrychia calliptera* (**A**) and *B. montagnei* (**B**) measured every 24 h during incubation (72 h) of the macroalgae under a range of salinities (5.1, 11.2, 18.4, 37.1, 47.1, and 57.3 $S_A$). Symbols are means with standard deviation (bars) based on six replicates

Based on rETR vs. PAR curves (Fig. 2), clear species-specific photosynthetic performance patterns were observed. *Bostrychia calliptera* decreased its photosynthetic performance under 37.1, 47.1, and 57.3 $S_A$, and *B. montagnei* under 47.1 and 57.3 $S_A$ (Fig. 2). In relation to the photosynthetic parameters calculated from the rETR vs. PAR curves, *B. calliptera* decreased the light utilization coefficient (α) and maximum relative electron transport rates ($rETR_{max}$) under increased salinity (Table 1). Although higher

**Table 1** Maximum quantum yield ($F_v/F_m$) and photosynthetic parameters from the relative electron transport rate vs. photon fluence rate curves of *Bostrychia calliptera* and *B. montagnei* incubated under different salinities ($S_A$) after 72 h

| Species | Salinity | $F_v/F_m$ | α (e photons$^{-1}$) | β (e photons$^{-1}$) | $rETR_{max}$ (μmol e m$^{-2}$ s$^{-1}$) | $I_k$ (μmol e m$^{-2}$ s$^{-1}$) |
|---|---|---|---|---|---|---|
| *B. calliptera* | 5.1 | $0.604 \pm 0.03^{a}$ | $0.125 \pm 0.01^{a}$ | $-0.0004 \pm 0.00^{a}$ | $11.15 \pm 4.16^{a}$ | $89.01 \pm 29.35^{a}$ |
| | 11.2 | $0.607 \pm 0.03^{a}$ | $0.117 \pm 0.05^{a}$ | $-0.0008 \pm 0.00^{ab}$ | $8.25 \pm 0.98^{a}$ | $82.12 \pm 9.79^{a}$ |
| | 18.4 | $0.620 \pm 0.02^{a}$ | $0.118 \pm 0.01^{a}$ | $-0.0007 \pm 0.00^{ab}$ | $10.15 \pm 2.68^{a}$ | $91.15 \pm 30.33^{a}$ |
| | 37.1 | $0.502 \pm 0.03^{b}$ | $0.104 \pm 0.01^{ab}$ | $-0.003 \pm 0.00^{b}$ | $3.83 \pm 1.17^{b}$ | $36.30 \pm 10^{b}$ |
| | 47.1 | $0.447 \pm 0.02^{c}$ | $0.042 \pm 0.00^{b}$ | $-0.001 \pm 0.00^{ab}$ | $2.35 \pm 0.17^{b}$ | $54.82 \pm 4.05^{ab}$ |
| | 57.3 | $0.450 \pm 0.03^{c}$ | $0.068 \pm 0.00^{b}$ | $-0.003 \pm 0.00^{ab}$ | $4.30 \pm 2.34^{b}$ | $63.24 \pm 34.41^{ab}$ |
| *B. montagnei* | 5.1 | $0.619 \pm 0.00^{A}$ | $0.176 \pm 0.06^{A}$ | $-0.003 \pm 0.00^{A}$ | $18.22 \pm 2.88^{A}$ | $107.99 \pm 19.48^{AB}$ |
| | 11.2 | $0.596 \pm 0.03^{AB}$ | $0.170 \pm 0.03^{A}$ | $-0.003 \pm 0.00^{A}$ | $18.36 \pm 2.86^{A}$ | $110.65 \pm 27.94^{AB}$ |
| | 18.4 | $0.602 \pm 0.01^{AB}$ | $0.154 \pm 0.02^{A}$ | $-0.001 \pm 0.00^{B}$ | $16.98 \pm 2.11^{A}$ | $111.03 \pm 14.15^{AB}$ |
| | 37.1 | $0.567 \pm 0.01^{B}$ | $0.133 \pm 0.02^{A}$ | $-0.0006 \pm 0.00^{B}$ | $19.03 \pm 5.55^{A}$ | $143.11 \pm 35.23^{A}$ |
| | 47.1 | $0.473 \pm 0.03^{C}$ | $0.146 \pm 0.01^{A}$ | $-0.003 \pm 0.00^{AB}$ | $11.93 \pm 2.93^{AB}$ | $83.78 \pm 24.46^{BC}$ |
| | 57.3 | $0.451 \pm 0.03^{C}$ | $0.135 \pm 0.02^{A}$ | $-0.0008 \pm 0.00^{B}$ | $7.58 \pm 2.05^{B}$ | $57.16 \pm 15.76^{C}$ |

α and β are the light utilization and photoinhibition coefficients, respectively. $rETR_{max}$ is the maximum relative electron transport rate and $I_k$ is the saturation irradiance for photosynthesis. Values are means with standard deviations based on six replicates ($n=6$). Different lowercase and uppercase letters represent significant differences ($P<0.05$) among treatments of salinity variation for *B. calliptera* and *B. montagnei*, respectively, by one-way ANOVA or Kruskal–Wallis test (Table S1) and Tukey or Dunn post hoc test, respectively

photoinhibition coefficient (β) values and lower saturation irradiance for photosynthesis ($I_k$) values of *B. calliptera* have been observed under increased salinity, a significant difference was only found at 37.1 $S_A$ (Table 1). For *B. montagnei*, a significant effect of increased salinity on α was not observed, whereas the $rETR_{max}$ and $I_k$ decreased at 57.3 $S_A$ (Table 1). A clear pattern in β among the salinity treatments for *B. montagnei* was not found (Table 1). Between species, *B. montagnei* exhibited higher α, $rETR_{max}$, and $I_k$ than *B. calliptera* (Table 1), whereas β was similar between species ($W=798$, $P=0.09$).

Analyzing the complementary energy dissipation pathways in PSII of both macroalgae, *B. calliptera* decreased the Y(II) under 37.1, 47.1, and 57.3 $S_A$ (Fig. 3A). The Y(NPQ) differed only between 11.2 and 47.1 $S_A$, and the Y(NO) increased under 37.1, 47.1, and 57.3 $S_A$ (Fig. 3A). *Bostrychia montagnei* decreased the Y(II) and increased the Y(NO) under 47.1 and 57.3 $S_A$ (Fig. 3B). Its lowest Y(NPQ) was observed at 47.1 $S_A$, thereby differing from those observed at 11.2 and 37.1 $S_A$ (Fig. 3B). Between species, *B. montagnei* showed higher Y(II) than *B. calliptera* ($0.39 \pm 0.06 > 0.32 \pm 0.09$; $W=338$, $P=0.003$). *Bostrychia calliptera* revealed higher Y(NPQ) than *B. montagnei* ($0.11 \pm 0.02 > 0.08 \pm 0.02$; $t=6.40$, $P<0.001$), and the Y(NO) was similar between *B. calliptera* and *B. montagnei* ($W=725$, $P=0.38$).

## Biochemical responses

The main organic osmolyte identified and quantified in *B. calliptera* was dulcitol, which increased at 37.1, 47.1, and 57.3 $S_A$ (Fig. 4A). Overall, the dulcitol content in *B. calliptera* doubled across these three salinities. Sorbitol was only identified and quantified as trace compound in *B. calliptera* at 37.1, 47.1, and 57.3 $S_A$ (Fig. 4A). A significant 2.5-times increase of sorbitol in *B. calliptera* was observed between 37.1 and 57.3 $S_A$ (Fig. 4A). *Bostrychia montagnei* synthesized both organic osmolytes dulcitol and sorbitol under the six salinities (Fig. 4B). The increase in salinity was accompanied by an increase of dulcitol and sorbitol in *B. montagnei* (Fig. 4B). At 57.3 $S_A$, the dulcitol and sorbitol contents in *B. montagnei* increased about 5.5 and 8.5-times, respectively, in relation to 5.1 $S_A$. Between species, *B. calliptera* revealed a higher dulcitol content than *B. montagnei* ($W=1268$, $P<0.001$), whereas *B. montagnei* contained a higher sorbitol content than *B. calliptera* ($W=36$, $P<0.001$; Fig. 4).

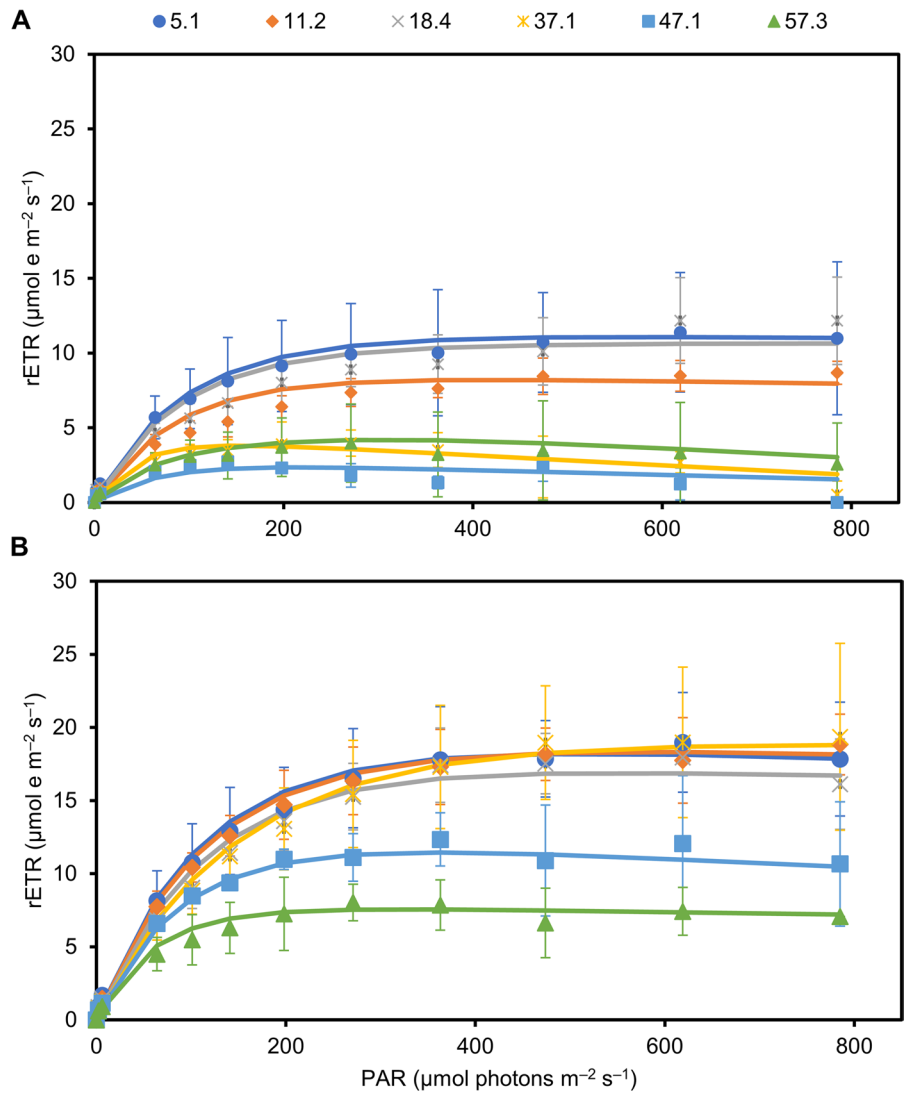


**Fig. 2** Relative electron transport rate (rETR) vs. photon fluence rate (PAR) curves of *Bostrychia calliptera* (**A**) and *B. montagnei* (**B**) incubated under a range of salinities (5.1, 11.2, 18.4, 37.1, 47.1, and 57.3 $S_A$) for 72 h. Symbols are mean measured rETRs with standard deviation (bars) for each salinity treatment based on six replicates. Lines are rETR vs. PAR curves fitted applying the mathematical model of Walsby (1997) for each salinity treatment

## Discussion

Increased salinity in tropical estuarine environments due to climate change will have detrimental effects on the photosynthetic performance of *B. calliptera* and *B. montagnei*. In our study, the negative effect of hypersaline conditions on the effective and maximum quantum yield of the macroalgae demonstrates that high salinities decrease the efficiency with which the PSII reaction centers capture and utilize excitation energy in photochemistry (Genty et al., 1989). In a previous study, *B. calliptera* and *B. montagnei* from tropical and subtropical mangroves of Brazil also showed a decline of their effective quantum yield when subjected to 25 and 35 $S_A$ compared to 15 $S_A$ (Borburema et al. 2022b). A negative effect of increased salinity on the quantum yield of other macroalgal species was also previously reported, for example, for *Champia novae-zelandiae* (Hooker f. & Harvey) Harvey and *Schizymenia* sp. (Gambichler et al., 2021a), *Pyropia plicata* W. A. Nelson (Diehl et al., 2019), and *Ulva pertusa* Kjellman (Choi et al., 2010). However, the maximum quantum yield of *Bostrychia arbuscula* W. H. Harvey from New Zealand was not affected by salt stress, pointing to a broad salinity tolerance of that particular *Bostrychia* species (Gambichler et al., 2021a). Emersion periods are relevant for *Bostrychia* species to capture

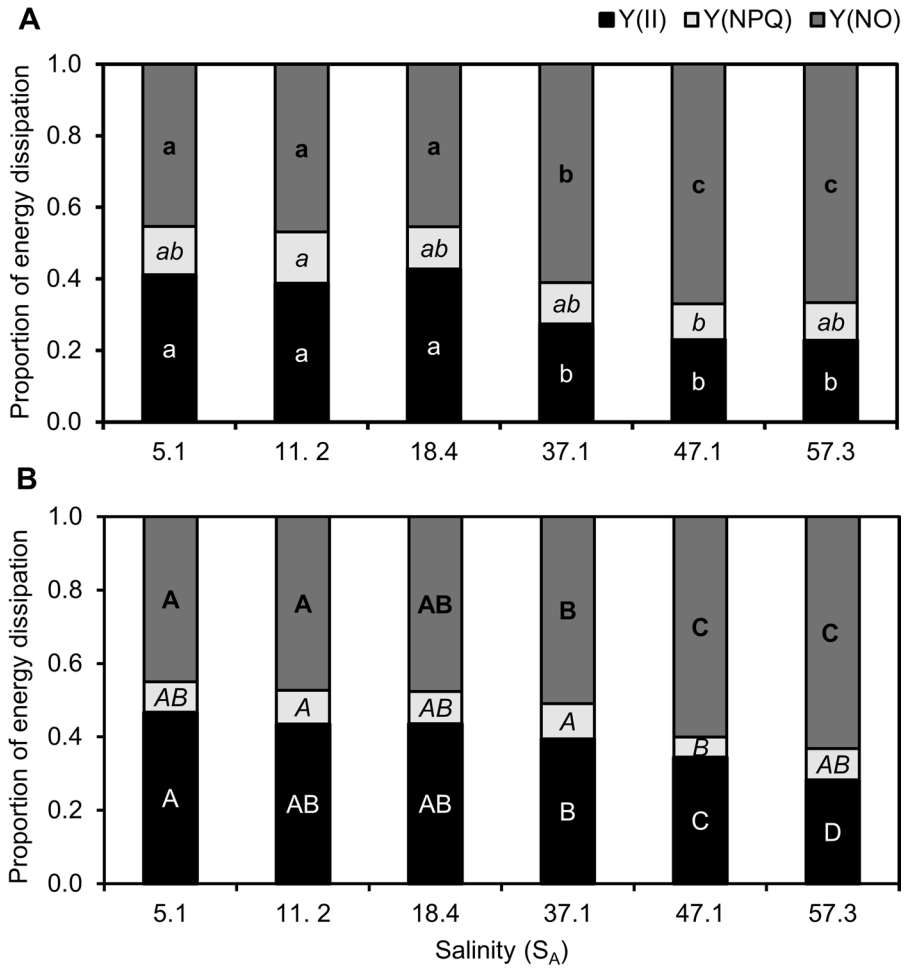


**Fig. 3** Complementary energy dissipation pathways in photosystem II of *Bostrychia calliptera* (**A**) and *B. montagnei* (**B**) incubated under a range of salinities (5.1, 11.2, 18.4, 37.1, 47.1, and 57.3 $S_A$) for 72 h. Y(II) is the photochemical pathway, Y(NPQ) is the regulated non-photochemical quenching of light energy, and Y(NO) is the non-regulated non-photochemical quenching of light energy. Columns are mean proportions based on six replicates. Different regular, italic, and bold lowercase letters indicate statistical differences for Y(II), Y(NPQ), and Y(NO), respectively, among salinity treatments for *B. calliptera*; whereas different regular, italic, and bold uppercase letters indicate statistical differences for Y(II), Y(NPQ), and Y(NO), respectively, among salinity treatments for *B. montagnei*. The statistical differences were found applying one-way ANOVA or Kruskal–Wallis' test (Table S1) followed by associated post hoc tests

atmospheric $CO_2$ (Mercado & Niell, 2000). Nevertheless, higher photosynthetic activity in *B. calliptera* has been documented under submersed conditions (Peña et al., 1999). In our study, the maximum quantum yield of both species under lower salinities was similar to that reported in *B. arbuscula* under field conditions (Gambichler et al., 2021a) and to that documented in *B. scorpioides* under lowest desiccation stress (Sánchez de Pedro et al., 2022). Thus, continuous submersed conditions during the acclimation period certainly did not result in carbon limitation. Furthermore, under higher salinities both species increased their polyol contents, whose chemical structure is based on carbon.

Several studies have demonstrated that *Bostrychia* species are euryhaline, as they are tolerant to wide ranges of salinity (Mann & Steinke, 1988; Karsten & Kirst, 1989a; Karsten et al., 1993, 1994a, b, 1995). Based on these reports, studies performed with Brazilian specimens confirmed the euryhaline nature of the genus *Bostrychia* (i.e., Borburema et al., 2020, 2022b). In the present study, *B. calliptera* and

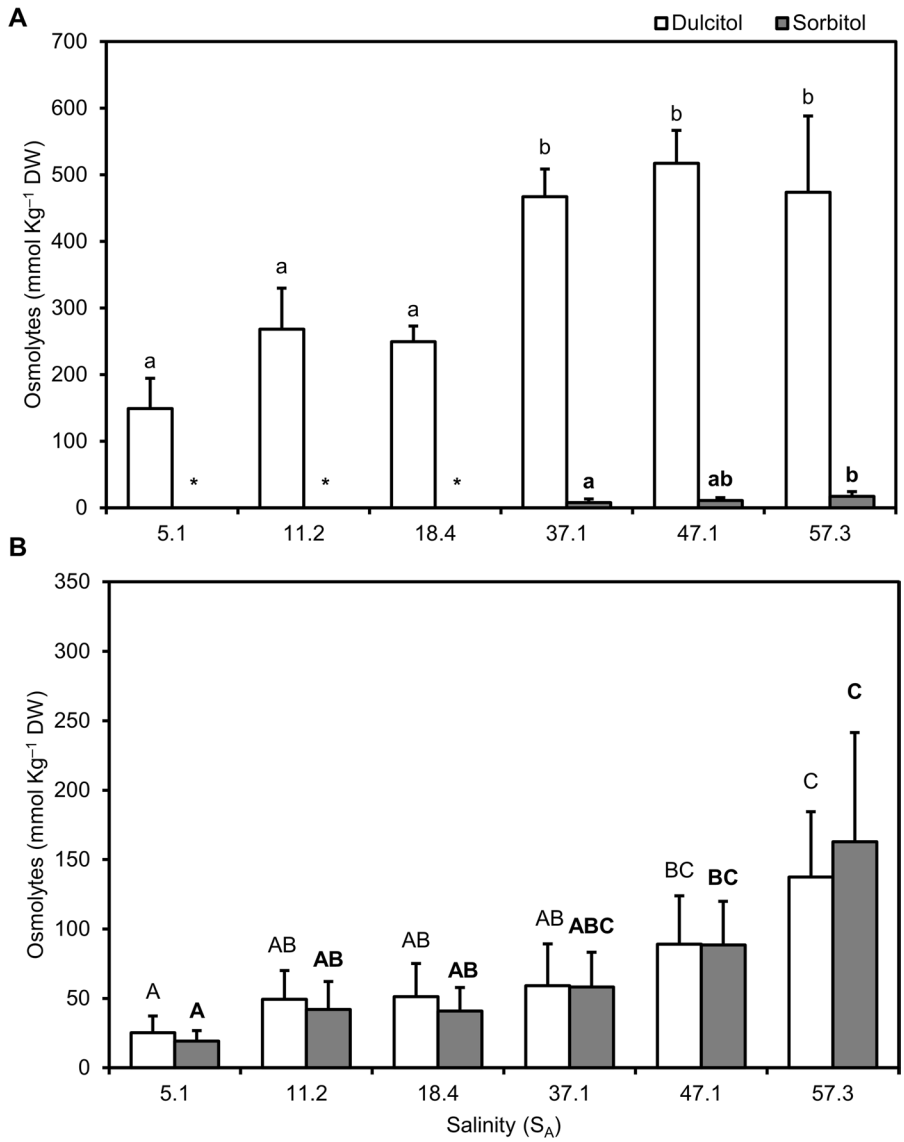


**Fig. 4** Organic osmolyte content (mmol $Kg^{-1}$ dry weight, DW) in *Bostrychia calliptera* (**A**) and *B. montagnei* (**B**) incubated under a range of salinities (5.1, 11.2, 18.4, 37.1, 47.1, and 57.3 $S_A$) for 72 h. Columns are means and bars are standard deviations based on six replicates. Different regular and bold lowercase letters indicate statistical differences for dulcitol and sorbitol, respectively, among salinity treatments for *B. calliptera*; whereas different regular and bold uppercase letters indicate statistical differences for dulcitol and sorbitol, respectively, among salinity treatments for *B. montagnei*. The statistical differences were found applying one-way ANOVA or Kruskal–Wallis' test (Table S1) followed by associated post hoc tests

*B. montagnei* were also characterized as euryhaline, since they showed photosynthetic activity under salinities from 5.1 to 57.3 $S_A$ and exhibited osmotic acclimation by synthesizing and accumulating organic osmolytes under salt stress or by degrading them under hyposaline conditions. Dulcitol and sorbitol are low molecular weight carbohydrates of the hexitol type that can be used as respiratory substrates (Kremer, 1976). A lower photosynthetic performance of both species was observed under higher salinities, mainly in *B. calliptera*. In Mamanguape river estuary, the mean salinity varies from 3.2 $S_A$ in the upper parts to 38.2 $S_A$ near the estuarine mouth (Lima et al., 2020). Thus, it was expected that both *Bostrychia* species exhibit a lower photosynthetic performance under hypersaline conditions of 47.1 and 57.3 $S_A$. Studies on the spatial distribution of both species along the estuary are still lacking.

The lower relative electron transport rates (rETRs) in *B. calliptera* were measured under salinities of 37.1, 47.1, and 57.3 $S_A$, and the lower rETRs in *B. montagnei* were determined at 47.1 and 57.3 $S_A$. This photobiological response refers to the linear electron flow through the PSII reaction centers (Genty et al., 1989; Suggett et al., 2011). Commonly, high salinities inhibit the electron flow at the PSII reaction centers,

as well as the transfer of light energy among pigment complexes (Kirst, 1990). Red macroalgae, such as *Bostrychia* species, have phycobiliproteins (phycoerythrin, phycocyanin, and allophycocyanin) and carotenoids as accessory pigments, which capture and transfer light energy toward chlorophyll *a* (Talarico, 1996; Lalegerie et al., 2019). Therefore, higher salinities may also have inhibited the transfer of light energy among pigment complexes (i.e., accessory pigments) toward chlorophyll *a* in both species, but mainly in *B. calliptera*, as it showed a decrease in rETRs at 37.1 $S_A$ as well. Photosynthetic parameters derived from the rETR vs. PAR curves also demonstrated the negative effect of hypersaline conditions on the photosynthetic performance of both macroalgae. The light utilization coefficient (α) and the maximum relative electron transport rates ($rETR_{max}$) of *B. calliptera* were lower at 47.1 and 57.3 $S_A$, and the $rETR_{max}$ and the saturation irradiance for photosynthesis ($I_k$) of *B. montagnei* were lower at 57.3 $S_A$. Mann and Steinke (1988) also observed a decrease in photosynthetic rates—measured as photosynthetic oxygen evolution—of *Bostrychia binderi* Harvey from a South African mangrove swamp under hypersaline condition (45 $S_A$). Other studies also reported an inhibition in algal photosynthetic performance under short-term as well as long-term hyperosmotic stresses (e.g., Kirst, 1981; Reed, 1983; Borlongan et al., 2016). However, Karsten & Kirst (1989a) reported an increase in photosynthesis of *Bostrychia radicans* (Montagne) Montagne under salinities of 28.9 and 37.4 $S_A$, when compared to 9.9 and 19.4 $S_A$. The increased photosynthetic activity of *B. radicans* shown by those authors could be related to moderate physiological stress due to the higher salinities. Usually, macroalgae up-regulate their metabolism to synthesize protective metabolites under increasing stressful conditions (Lesser, 2006; Gambichler et al., 2021b).

*Bostrychia montagnei* revealed a similar light utilization coefficient among salinities, which reinforces its greater tolerance to osmotic stress than *B. calliptera*. The absence of a clear negative effect of increased salinity on the photoinhibition coefficient (β) indicates that photoinhibition in both species was not influenced by salinity. This is in agreement with the minor inhibition of photosynthesis in the closely related *B. radicans* subjected to hyperosmotic shock (Karsten & Kirst, 1989a). Concerning the saturation irradiance for photosynthesis ($I_k$), both species can be characterized as typical "shade plants," since they exhibited saturated photosynthesis under low photon fluence rates (*B. calliptera* 36.3–91.2 µmol electrons $m^{-2}$ $s^{-1}$, *B. montagnei* 57.2–143.1 µmol electrons $m^{-2}$ $s^{-1}$). These results are consistent with several studies on numerous other *Bostrychia* species, which were always characterized as typical "shade plants', because of the low light requirements for photosynthesis (Karsten & Kirst, 1989a; Karsten et al., 1993, 1994a, b; Sánchez de Pedro et al., 2014). This physiological characteristic of *Bostrychia* species is directly related to their preferential occurrence in shaded habitats, such as mangrove swamps and salt marshes, where they are protected from full sun exposure by the covering canopy (Karsten et al., 1994a). Environmental and ecological data support this shade preference of both species. The mean irradiance on the algal collection area is around 220 W $m^{-2}$ (INPE, 2022), which corresponds to about 1012 µmol photons $m^{-2}$ $s^{-1}$ (Lüning, 1990). After attenuation by the covering canopy, the mean proportions of incident irradiance on the Bostrychietum of Brazilian mangroves are around 5, 8, and 17% (Yokoya et al., 1999b), which corresponds to photon fluence rates of around 51, 81, and 173 µmol photons $m^{-2}$ $s^{-1}$, respectively. Those proportions of incident light varied depending on the density of the covering canopy. Our results from the complementary energy dissipation pathways are congruent with our results from the rETR vs. PAR curves. Both species showed a lower use of light energy at the PSII reaction centers (Y[II]) under increased salinity, whereas revealed a higher non-regulated non-photochemical quenching of light energy (Y[NO]) under hyperosmotic stress. Thus, increased Y(NO) at the expense of Y(II) suggests photoinhibition or permanent destruction of the photosynthetic apparatus (Klughammer & Schreiber, 2008; Graiff et al., 2021). The hyperosmotic stress in general may have resulted in harmful effects on the algal photosynthetic apparatus, leading to a lower photophysiological performance of both species under those conditions.

Organic osmolytes, dulcitol and sorbitol, were synthesized and accumulated by *B. montagnei* for osmotic acclimation under salt stress, while under hyposaline conditions, they were degraded. Similar findings have been reported by several studies in which other *Bostrychia* species were subjected to

osmotic stress (Karsten et al. 1993, 1994a, b, 1995, 1996a, b; Gambichler et al., 2021a). Surprisingly, in *B. calliptera* the main organic osmolyte was dulcitol. Sorbitol was only synthesized and accumulated under rising salinities between 37.1 and 57.3 $S_A$, however, in relatively low concentrations. Under lower salinities between 5.1 and 18.4 $S_A$, only dulcitol was identified and quantified. Organic osmolytes such as polyols exert further biochemical functions as they can act as compatible solutes (protect enzymes and structural molecules), i.e., these compounds are highly soluble in the cytoplasm and non-toxic at high concentrations (Kirst, 1990). Biosynthesis and accumulation of compatible solutes under rising osmotic stress permits the generation of low water potentials without resulting in metabolic damages such as the inactivation, inhibition, and denaturation of enzymes (Kirst, 1990). Historically, only two organic osmolyte distribution patterns have been observed in *Bostrychia* species: sorbitol plus dulcitol, or sorbitol only, i.e., the sole occurrence of dulcitol has never been observed (based on the previously referenced literature). The biosynthesis of only one organic osmolyte involves less enzymatic steps and thus saves metabolic energy. Moreover, the presence of only one organic osmolyte (i.e., sorbitol as reported in the literature until now) would be fully sufficient for osmotic acclimation in *Bostrychia* species (Karsten et al., 1994b). Based on several studies (previously referenced literature), there is the assumption that sorbitol is the dominant and regulated saline stress protective compound in *Bostrychia* species, while dulcitol does not seem to play a major role as actively adjusted osmolyte. This assumption is also based on physicochemical differences between sorbitol and dulcitol. Sorbitol has a 25-times higher solubility in water than dulcitol (sorbitol, 4.6 M; dulcitol, 0.18 M) (Lide, 1992), thus, it can be a much better osmolyte than dulcitol (Karsten et al., 1994a, 1994b). However, our findings, i.e., the sole occurrence of dulcitol in *B. calliptera* at lower salinities, and as the main organic osmolyte in this species at higher salinities, do not support this assumption. In addition, our data are corroborated by Karsten et al. (1992) who identified and quantified mainly dulcitol in field samples of *B. calliptera* from Brazil (45–95 µmol $g^{-1}$ DW of dulcitol and very low levels of sorbitol, 3–7 µmol $g^{-1}$ DW). Thus, we recognized a third organic osmolyte distribution pattern in *Bostrychia* species, i.e., dulcitol only. Enzymological and metabolomic data on *Bostrychia* species (which are still missing) are needed to better understand the metabolic pathways for the biosynthesis of organic osmolytes in *Bostrychia* species, and Brazilian lineages are strong candidates to be used as model organisms.

In conclusion, our hypotheses were confirmed, since (i) increased salinity was detrimental to macroalgal photosynthesis; (ii) both species revealed osmotic acclimation in response to the increase in salinity by synthesizing and accumulating organic osmolytes, sorbitol, and/or dulcitol; and (iii) *B. calliptera* showed a lower physiological performance than *B. montagnei* under increased salinity. This difference between species can be explained because *B. montagnei* synthesizes both dulcitol and sorbitol under saline stress, and that sorbitol is a physicochemically better organic osmolyte than dulcitol (Karsten et al., 1994a, b). Therefore, although both species exhibited osmotic acclimation under hypersaline conditions, confirming their euryhaline nature, increased salinity in tropical estuarine environments influenced by semi-arid climate will be detrimental to photosynthesis of *B. calliptera* and *B. montagnei*. Osmotic acclimation in macroalgal species results in high energy expenditure (Kirst, 1990; Karsten, 2012). Thus, photosynthesis of *Bostrychia* species negatively affected by hyperosmotic stress may compromise their osmotic acclimation and populational fitness. The incubation time (i.e., 72 h) for both species under different salinities was sufficient for an osmotic acclimation, confirming data observed by Karsten et al. (1994a, b, 1996a). In the climate change context, algal desiccation due to the long emersion periods can be an additive environmental stressor to the saline stress (Peña et al., 1999; Sánchez de Pedro et al., 2022), as well as the increase in temperature (Borburema et al., 2022b). Future field studies exploring the spatial and temporal distribution and vertical zonation patterns of both *Bostrychia* species are needed to better predict the impact of salinity change on the dynamic of macroalgae in the mangrove swamp. Biochemical and genomic studies are also needed to elucidate the metabolic pathways of dulcitol and sorbitol, which result in three organic osmolyte distribution patterns in *Bostrychia* species: sorbitol together with

dulcitol, sorbitol only, and dulcitol only. The latter reported for the first time in our study.

**Acknowledgements** We are grateful to Niklas Plag (University of Rostock, Applied Ecology and Phycology) for the technical support during dulcitol and sorbitol analyses by HPLC. H.D.S. Borburema is grateful to the Coordination for the Improvement of Higher Education Personnel (CAPES-Brazil) by funding his stay at University of Rostock (Germany) for research activities (Finance code: 88887.586537/2020-00). We thank the anonymous reviewers and our editor Dr. Sally Entrekin for their constructive comments that greatly improved the manuscript.

**Funding** This study was financed in part by the Coordenação de Aperfeiçoamento de Pessoal de Nível Superior—Brasil (CAPES)—Finance Code 001 and 88887.586537/2020-00, Ph.D. fellowships for H.D.S. Borburema. This study was also supported within the framework of the Research Training Group Baltic TRANSCOAST funded by the DFG (Deutsche Forschungsgemeinschaft) under grant number GRK 2000/1. This is Baltic TRANSCOAST publication no. GRK2000/00XY).

**Data availability** The datasets generated during and/or analyzed during the current study are available from the corresponding author on reasonable request.

**Declarations**

**Conflict of interest** The authors declare they have no conflict of interests.

## References

Alvares, C. A., J. L. Stape, P. C. Sentelhas, J. L. De Moraes Gonçalves & G. Sparovek, 2013. Köppen's climate classification map for Brazil. Meteorologische Zeitschrift 22: 711–728.

Bindoff, N. L., W. W. L. Cheung, J. G. Kairo, J. Arístegui, V. A. Guinder, R. Hallberg, N. Hilmi, N. Jiao, M. S. Karim, L. Levin, S. O'Donoghue, S. R. Purca Cuicapusa, B. Rinkevich, T. Suga, A. Tagliabue, & P. Williamson, 2019. Changing Oean, Marine Ecosystems, and Dependent Communities In Pörtner, H.-O., D. C. Roberts, V. Masson-Delmotte, P. Zhai, M. Tignor, E. Poloczanska, K. Mintenbeck, A. Alegría, M. Nicolai, A. Okem, J. Petzold, B. Rama, & N. M. Weyer (eds), IPCC Special Report: The Ocean and Cryosphere in a Changing Climate. In press: 447–587, https://www.ipcc.ch/srocc/download-report/.

Borburema, H. D. S., R. P. Lima & G. E. C. Miranda, 2020. Effects of ocean warming, eutrophication and salinity variations on the growth of habitat-forming macroalgae in estuarine environments. Acta Botanica Brasilica 34: 662–672.

Borburema, H. D. S., Ê. N. A. Barbosa & G. E. C. Miranda, 2021. Decontamination protocol of the macroalga *Bostrychia binderi* Harvey (Rhodophyta) for unialgal cultures and laboratory studies. Hoehnea 48: e582020.

Borburema, H. D. S., N. S. Yokoya, L. P. Soares, J. M. C. Souza, F. Nauer, M. T. Fujii, C. B. Pasqualetii, G. E. C. Miranda & E. Marinho-Soriano, 2022a. Mangrove macroalgae increase their growth under ocean acidification: a study with *Bostrychia* ( Rhodophyta ) haplotypes from different biogeographic provinces. Journal of Experimental Marine Biology and Ecology 552: 151740.

Borburema, H. D. S., N. S. Yokoya, J. M. C. Souza, F. Nauer, M. S. Barbosa-silva & E. Marinho-Soriano, 2022b. Ocean warming and increased salinity threaten *Bostrychia* (Rhodophyta) species from genetically divergent populations. Marine Environmental Research 178: 105662.

Borlongan, I. A. G., M. R. J. Luhan, P. I. P. Padilla & A. Q. Hurtado, 2016. Photosynthetic responses of '*Neosiphonia* sp. epiphyte-infected' and healthy *Kappaphycus alvarezii* (Rhodophyta) to irradiance, salinity and pH variations. Journal of Applied Phycology 28: 2891–2902.

Carneiro, M. A., do A., J. F. de J. Resende, S. R. Oliveira, F. de O. Fernandes, H. D. dos S. Borburema, M. S. Barbosa-Silva, A. B. G. Ferreira, & E. Marinho-Soriano, 2020. Performance of the agarophyte *Gracilariopsis tenuifrons* in a multi-trophic aquaculture system with *Litopenaeus vannamei* using water recirculation. Journal of Applied Phycology 33: 481–490.

Celis-Plá, P. S. M., J. M. Hall-Spencer, P. A. Horta, M. Milazzo, N. Korbee, C. E. Cornwall & F. L. Figueroa, 2015. Macroalgal responses to ocean acidification depend on nutrient and light levels. Frontiers in Marine Science 2: 26.

Choi, T.-S., E.-J. Kang, J.-H. Kim & K.-Y. Kim, 2010. Effect of salinity on growth and nutrient uptake of *Ulva pertusa* (Chlorophyta) from an eelgrass bed. Algae 25: 17–26.

Collins, M., R. Knutti, J. Arblaster, J.-L. Dufresne, T. Fichefet, P. Friedlingstein, X. Gao, W. J. Gutowski, T. Johns, G. Krinner, M. Shongwe, C. Tebaldi, A. J. Weaver, & M. Wehner, 2013. Long-term Climate Change: Projections, Commitments and Irreversibility In Stocker, T. F., D. Qin, G.-K. Plattner, M. Tignor, S. K. Allen, J. Boschung, A. Nauels, Y. Xia, V. Bex, & P. M. Midgley (eds), Climate Change 2013: The Physical Science Basis. Contribution of Working Group I to the Fifth Assessment Report of the Intergovernmental Panel on Climate Change. Cambridge University Press, Cambridge, United Kingdom and New York, NY, USA: 1029–1136.

Cunha, S. R. & C. S. Costa, 2002a. Gradientes de salinidade e freqüência de alagamento como determinantes da distribuição e biomassa de macroalgas associadas a troncos de manguezais na baía de babitonga, SC. Notas Técnicas Facimar 6: 93–102.

Cunha, S. R. & N. R. Duarte, 2002b. Taxas fotossintéticas e respiratórias de macroalgas do gênero *Bostrychia*. Notas Técnicas Facimar 6: 103–110.

Diehl, N., D. Michalik, G. C. Zuccarello & U. Karsten, 2019. Stress metabolite pattern in the eulittoral red alga *Pyropia plicata* (Bangiales) in New Zealand—mycosporine-like amino acids and heterosides. Journal of Experimental Marine Biology and Ecology 510: 23–30.

Duarte, R. C. S., G. Barros, S. V. Milesi & T. L. P. Dias, 2020. Influence of macroalgal morphology on the functional

structure of molluscan community from hypersaline estuary. Hydrobiologia 847: 1107–1119.
Figueroa, F. L., P. S. M. Celis-Plá, B. Martínez, N. Korbee, A. Trilla & F. Arenas, 2019. Yield losses and electron transport rate as indicators of thermal stress in *Fucus serratus* (Ochrophyta). Algal Research 41: 101560.
Fontes, K. A. A., S. M. B. Pereira & C. S. Zickel, 2007. Macroalgas do "Bostrychietum" aderido em pneumatóforos de duas áreas de manguezal do Estado de Pernambuco, Brasil. Iheringia—Serie Botanica 62: 31–38.
Gambichler, V., G. C. Zuccarello & U. Karsten, 2021a. Physiological responses to salt stress by native and introduced red algae in New Zealand. Algae 36: 137–146.
Gambichler, V., G. C. Zuccarello & U. Karsten, 2021b. Seasonal changes in stress metabolites of native and introduced red algae in New Zealand. Journal of Applied Phycology 33: 1157–1170.
García, A. F., M. Bueno & F. P. P. Leite, 2016. The Bostrychietum community of pneumatophores in Araçá Bay: An analysis of the diversity of macrofauna. Journal of the Marine Biological Association of the United Kingdom 96: 1617–1624.
Genty, B., J. M. Briantais & N. R. Baker, 1989. The relationship between the quantum yield of photosynthetic electron transport and quenching of chlorophyll fluorescence. Biochimica Et Biophysica Acta 990: 87–92.
Giri, C., E. Ochieng, L. L. Tieszen, Z. Zhu, A. Singh, T. Loveland, J. Masek & N. Duke, 2011. Status and distribution of mangrove forests of the world using earth observation satellite data. Global Ecology and Biogeography 20: 154–159.
Gonçalves, C. T. P., 2020. Florações de macroalgas e seus efeitos sobre a pesca e macrofauna em uma região neotropical. PhD Thesis. Universidade Federal do Rio Grande do Norte.
Graiff, A., I. Bartsch, K. Glaser & U. Karsten, 2021. Seasonal photophysiological performance of adult Western Baltic *Fucus vesiculosus* (Phaeophyceae) under ocean warming and acidification. Frontiers in Marine Science 8: 666493.
INPE, 2022. Instituto Nacional de Pesquisas Espaciais. Divisão de Satélites e Sistemas Ambientais. http://satelite.cptec.inpe.br/radiacao/.
IPCC, 2014. Climate Change 2014: Synthesis Report. Contribution of Working Groups I, II and III to the Fifth Assessment Report of the Intergovernmental Panel on Climate Change. IPCC, Geneva, Switzerland.
IPCC, 2019. Summary for policymakers In Pörtner, H.-O., D. C. Roberts, V. Masson-Delmotte, P. Zhai, M. Tignor, E. Poloczanska, K. Mintenbeck, A. Alegría, M. Nicolai, A. Okem, J. Petzold, B. Rama, & N. M. Weyer (eds), IPCC Special Report on the Ocean and Cryosphere in a Changing Climate. In press: 1–34, http://www.gtp89.dial.pipex.com/AR4.htm.
Karsten, U., 2012. Seaweed acclimation to salinity and desiccation stress. In Wiencke, C. & K. Bischof (eds), Seaweed Biology: Novel Insights into Ecophysiology, Ecology and Utilization. Springer, Berlin: 87–107.
Karsten, U. & G. O. Kirst, 1989a. The effect of salinity on growth, photosynthesis and respiration in the estuarine red alga *Bostrychia radicans*. Helgolander Meresunters 43: 61–66.
Karsten, U. & G. O. Kirst, 1989b. Incomplete turgor pressure regulation in the "terrestial" red alga, *Bostrychia scorpioides* (Huds.) Mont. Plant Science 61: 29–36.
Karsten, U., D. N. Thomas, G. Weykam, C. Daniel & G. O. Kirst, 1991. A simple and rapid method for exctraction and separation of low molecular weight carbohydrates from macroalgae using high-performance liquid chromatography. Plant Physiology and Biochemistry 29: 373–378.
Karsten, U., J. A. West & G. Zuccarello, 1992. Polyol content of *Bostrychia* and *Stictosiphonia* (Rhodomelaceae, Rhodophyta) from field and culture. Botanica Marina 35: 11–20.
Karsten, U., J. A. West & E. K. Ganesan, 1993. Comparative physiological ecology of *Bostrychia moritziana* (Ceramiales, Rhodophyta) from freshwater and marine habitats. Phycologia 32: 401–409.
Karsten, U., S. Koch, J. A. West & G. O. Kirst, 1994a. The intertidal red alga *Bostrychia simpliciuscula* Harvey ex J. Agardh from a mangrove swamp in Singapore: acclimation to light and salinity. Aquatic Botany 48: 313–323.
Karsten, U., J. A. West, G. C. Zuccarello & G. O. Kirst, 1994b. Physiological ecotypes in the marine alga *Bostrychia radicans* (Ceramiales, Rhodophyta) from the east coast of the U.S.A. Journal of Phycology 30: 174–182.
Karsten, U., C. Bock & J. A. West, 1995. Low molecular weight carbohydrate patterns in geographically different isolates of the eulittoral red alga *Bostrychia tenuissima* from Australia. Botanica Acta 108: 321–326.
Karsten, U., S. Koch, G. O. Kirst & J. A. West, 1996a. Physiological responses of the eulittoral macroalga *Stictosiphonia hookeri* (Rhodomelaceae, Rhodophyta) from Argentina and Chile: salinity, light and temperature acclimation. European Journal of Phycology 31: 361–368.
Karsten, U., A. S. Mostaerti, R. J. King, M. Kamiya & Y. Hara, 1996b. Osmoprotectors in some species of Japanese mangrove macroalgae. Phycological Research 44: 109–112.
Karsten, U., T. Sawall, J. West & C. Wiencke, 2000. Ultraviolet sunscreen compounds in epiphytic red algae from mangroves. Hydrobiologia 1: 159–171.
Kieckbusch, D. K., M. S. Koch, J. E. Serafy & W. T. Anderson, 2004. Trophic linkages among primary producers and consumers in fringing mangroves of subtropical lagoons. Bulletin of Marine Science 74: 271–285.
Kirst, G. O., 1981. Photosynthesis and respiration of *Griffithsia monilis* (Rhodophyceae): effect of light, salinity, and oxygen. Planta 151: 281–288.
Kirst, G. O., 1990. Salinity tolerance of eukaryotic marine algae. Annual Review of Plant Physiology and Plant Molecular Biology 41: 21–53.
Klughammer, C. & U. Schreiber, 2008. Complementary PS II quantum yields calculated from simple fluorescence parameters measured by PAM fluorometry and the Saturation Pulse method. PAM Application Notes 1: 27–35.
Kremer, B. P., 1976. 14C-Assimilate pattern and kinetics of photosynthetic $14CO_2$-assimilation of the marine red alga *Bostrychia scorpioides*. Planta 129: 63–67.
Lalegerie, F., S. Lajili, G. Bedoux, L. Taupin, V. Stiger-Pouvreau & S. Connan, 2019. Photo-protective compounds

in red macroalgae from Brittany: considerable diversity in mycosporine-like amino acids (MAAs). Marine Environmental Research 147: 37–48.
Lesser, M. P., 2006. Oxidative stress in marine environments: biochemistry and physiological ecology. Annual Review of Physiology 68: 253–278.
Lide, D. R., 1992. CRC Handbook of Chemistry and Physics. The Chemical Rubber Company, Cleveland: 2385.
Lima, C. S. S., M. L. A. S. Badú & A. L. M. Pessanha, 2020. Response of estuarine fish assemblages to an atypical climatic event in northeastern Brazil. Regional Studies in Marine Science 35: 101121.
Lüning, K., 1990. Seaweeds: Their Environment, Biogeography and Ecophysiology. Wiley, New York.
Machado, G. E. M. & C. A. G. Nassar, 2007. Assembléia de Macroalgas de dois manguezais do núcleo Picinguaba—Parque Estadual da Serra do Mar, São Paulo, Brasil. Rodriguésia 58: 835–846.
Mann, F. D. & T. D. Steinke, 1988. Photosynthetic and respiratory responses of the mangrove-associated red algae, *Bostrychia radicans* and *Caloglossa leprieurii*. South African Journal of Botany 54: 203–207.
Marengo, J. A., R. R. Torres & L. M. Alves, 2017. Drought in Northeast Brazil-past, present, and future. Theoretical and Applied Climatology 129: 1189–1200.
Melville, F. & A. Pulkownik, 2006. Investigation of mangrove macroalgae as bioindicators of estuarine contamination. Marine Pollution Bulletin 52: 1260–1269.
Melville, F. & A. Pulkownik, 2007. Investigation of mangrove macroalgae as biomonitors of estuarine metal contamination. Science of the Total Environment 387: 301–309.
Mendonça, I. R. W. & P. C. da Lana, 2021. Richness and biomass distribution of the mangrove macroalgal association in a subtropical estuary. Ocean and Coastal Research 69: e21032.
Mercado, J. M. & F. X. Niell, 2000. Carbon dioxide uptake by *Bostrychia scorpioides* (Rhodophyceae) under emersed conditions. European Journal of Phycology 35: 45–51.
Nauer, F., H. D. S. Borburema, N. S. Yokoya & M. T. Fujii, 2021. Effects of ocean acidification on growth, pigment contents and antioxidant potential of the subtropical Atlantic red alga *Hypnea pseudomusciformis* Nauer, Cassano & M.C. Oliveira (Gigartinales) in laboratory. Brazilian Journal of Botany 44: 69–77.
Nauer, F., M. C. Oliveira, E. M. Plastino, N. S. Yokoya & M. T. Fujii, 2022. Coping with heatwaves: how a key species of seaweed responds to heat stress along its latitudinal gradient. Marine Environmental Research 177: 105620.
Pedroche, F. F., J. A. West, G. C. Zuccarello & U. Karsten, 1995. Marine red Algae of the mangroves in pacific Mexico and Guatemala. Botanica Marina 38: 111–119.
Peña, E. J., R. Zingmark & C. Nietch, 1999. Comparative photosynthesis of two species of intertidal epiphytic macroalgae on mangrove roots during submersion and emersion. Journal of Phycology 35: 1206–1214.
Pereira, D. T., C. Simioni, E. P. Filipin, F. Bouvie, F. Ramlov, M. Maraschin, Z. L. Bouzon & É. C. Schmidt, 2017. Effects of salinity on the physiology of the red macroalga, *Acanthophora spicifera* (Rhodophyta, Ceramiales). Acta Botanica Brasilica 31: 555–565.
Post, E., 1936. Systematische und pflanzengeographische Notizen zur Bostrychia-Caloglossa Assoziation. Revue Algologie 9: 1–84.
Reed, R. H., 1983. The osmotic responses of *Polysiphonia lanosa* (L.) Tandy from marine and estuarine sites: evidence for incomplete recovery of turgor. Journal of Experimental Marine Biology and Ecology 68: 169–193.
Rios-Marin, F., E. J. Peña-Salamanca & R. Benítez-Benítez, 2021. Efecto del pH en las tasas de bioacumulación de metales pesados en la macroalga *Bostrychia calliptera* (Rhodomelaceae, Ceramiales). Acta Biológica Colombiana 26: 226–234.
Rybczyk, J. M., J. W. Day Jr., A. Yánez-Arancibia & J. H. Cowan, 2012. Global climate change and estuarine systems. In Day, J. W., Jr., B. C. Crump, W. M. Kemp & A. Yáñez-Arancibia (eds), Estuarine Ecology. Wiley-Blackwell, Singapore: 497–519.
Sales, N. D. S., A. S. B. V. Baeta, L. G. de Lima & A. L. M. Pessanha, 2018. Do the shallow water habitats of a hypersaline tropical estuary act as nursery grounds for fishes? Marine Ecology 39: e12473.
Sánchez de Pedro, R., F. X. Niell & R. Carmona, 2014. Understanding the intertidal zonation of two macroalgae from ex situ photoacclimation responses. European Journal of Phycology 49: 538–549.
Sánchez de Pedro, R., U. Karsten, F. X. Niell & R. Carmona, 2016. Intraspecific phenotypic variation in two estuarine rhodophytes across their intertidal zonation. Marine Biology 163: 221.
Sánchez de Pedro, R., F. X. Niell & R. Carmona, 2022. Close but distant: emersion promotes ecophysiological differentiation between two rhodophytes within an estuarine intertidal zone. Journal of Experimental Marine Biology and Ecology 547: 151664.
Sassi, R., M. B. B. Kutner & G. F. Moura, 1988. Studies on the decomposition of drift seaweed from the northeast Brazilian coastal reefs. Hydrobiologia 157: 187–192.
Scherner, F., R. Ventura, J. B. Barufi & P. A. Horta, 2013. Salinity critical threshold values for photosynthesis of two cosmopolitan seaweed species: providing baselines for potential shifts on seaweed assemblages. Marine Environmental Research 91: 14–25.
Scherner, F., C. M. Pereira, G. Duarte, P. A. Horta, C. B. E. Castro, J. B. Barufi & S. M. B. Pereira, 2016. Effects of ocean acidification and temperature increases on the photosynthesis of tropical reef calcified macroalgae. PLoS ONE 11: 1–14. https://doi.org/10.1371/journal.pone.0154844.
Schreiber, U., W. Bilger, & C. Neubauer. 1995. Chlorophyll-fluorescence as a nonintrusive indicator for rapid assessment of In vivo photosynthesis. In: Schulze, E.-D., & M. M. Caldwell(Eds.). Ecophysiology of Photosynthesis. Springer-Verlag: Berlin Heidelberg. 49–70.
Starr, R. & J. Zeikus, 1993. UTEX-the culture collection of algae at the University of Texas at Austin. Journal of Phycology 23(Suppl 2): 1–106.
Suggett, D. J., O. Prášil & M. A. Borowitzka, 2011. Chlorophyll *a* Fluorescence in Aquatic Sciences. Springer, Dordrecht.

Talarico, L., 1996. Phycobiliproteins and phycobilisomes in red algae: adaptive responses to light. Scientia Marina 60: 205–222.

Vieira, E. A., H. R. Filgueiras, M. Bueno, F. P. P. Leite & G. M. Dias, 2018. Co-occurring morphologically distinct algae support a diverse associated fauna in the intertidal zone of Araçá Bay, Brazil. Biota Neotropica 18: 1–8.

Walsby, A. E., 1997. Numerical integration of phytoplankton photosynthesis through time and depth in a water column. New Phytologist 136: 189–209.

West, J. A., G. C. Zuccarello, F. F. Pedroche & U. Karsten, 1992. Marine red algae of the mangroves in Pacific Mexico and their polyol content. Botanica Marina 35: 567–572.

Xavier, J. H. A., C. A. M. M. Cordeiros, G. D. Tenório, A. F. Diniz, E. P. N. P. Júnior, R. S. Rosa & I. L. Rosa, 2012. Fish assemblage of the Mamanguape Environmental Protection Area, NE Brazil: abundance, composition and microhabitat availability along the mangrove-reef gradient. Neotropical Ichthyology 10: 109–122.

Yokoya, N. S., H. Kakita, H. Obika & T. Kitamura, 1999a. Effects of environmental factors and plant growth regulators on growth of the red alga *Gracilaria vermiculophylla* from Shikoku Island. Japan. Hydrobiologia 398(399): 339–347.

Yokoya, N. S., E. M. Plastino, M. R. A. Braga, M. T. Fujii, M. Cordeiro-Marino, V. R. Eston & J. Harari, 1999b. Temporal and spatial variations in the structure of macroalgal communities associated with mangrove trees of Ilha do Cardoso, São Paulo state, Brazil. Revista Brasileira De Botânica 22: 195–204.